Journal of Power Sources 185 (2008) 280–286

Contents lists available at ScienceDirect

Journal of Power Sources

journal homepage: www.elsevier.com/locate/jpowsour

The influence of the electrochemical stressing (potential step and potential-static holding) on the degradation of polymer electrolyte membrane fuel cell electrocatalysts

Yuyan Shao, Rong Kou, Jun Wang, Vilayanur V. Viswanathan, Ja Hun Kwak, Jun Liu, Yong Wang, Yuehe Lin*

Pacific Northwest National Laboratory, Richland, WA 99352, United States

ARTICLE INFO

Article history:
Received 27 May 2008
Received in revised form 1 July 2008
Accepted 2 July 2008
Available online 17 July 2008

Keywords:
PEM fuel cell
Platinum
Electrocatalyst
Accelerated degradation test
Durability

ABSTRACT

The understanding of the degradation mechanisms of electrocatalysts is very important for developing durable electrocatalysts for polymer electrolyte membrane (PEM) fuel cells. The degradation of Pt/C electrocatalysts under potential-static holding conditions (at 1.2 V and 1.4 V vs. RHE) and potential step conditions with the upper potential of 1.4 V for 150 s and lower potential limits (0.85 V and 0.60 V) for 30 s in each period [denoted as Pstep(1.4V_150s–0.85V_30s) and Pstep(1.4V_150s–0.60V_30s), respectively] were investigated. The electrocatalysts and support were characterized with electrochemical voltammetry, transmission electron microscope (TEM) and X-ray photoelectron spectroscopy (XPS). Pt/C degrades much faster under Pstep conditions than that under potential-static holding conditions. Pt/C degrades under the Pstep(1.4V_150s–0.85V_30s) condition mainly through the coalescence process of Pt nanoparticles due to the corrosion of carbon support, which is similar to that under the conditions of 1.2 V- and 1.4 V-potential-static holding; however, Pt/C degrades mainly through the dissolution/loss and dissolution/redeposition process if stressed under Pstep(1.4V_150s–0.60V_30s). The difference in the degradation mechanisms is attributed to the chemical states of Pt nanoparticles: Pt dissolution can be alleviated by the protective oxide layer under the Pstep(1.4V_150s–0.85V_30s) condition and the potential-static holding conditions. These findings are very important for understanding PEM fuel cell electrode degradation and are also useful for developing fast test protocol for screening durable catalyst support materials.

1. Introduction

Recently, the research and development (R&D) of polymer electrolyte membrane (PEM) fuel cells and the component materials have shifted from their short-term performance to the durability and reliability to make fuel cells cost competitive [1–3]. Electrocatalysts and support materials are one of the most important factors that influence both the durability and cost of PEM fuel cells [2]. Much effort has been devoted to developing novel durable catalyst materials and elucidating the underlying nature of materials degradation in PEM fuel cells [1,2]. Presently, the most widely used electrocatalysts are still Pt-based ones. It has been found that Pt alloyed with other transition metals can improve both the activity and durability of electrocatalysts as compared with pure Pt [4,5]. Another method to produce a durable electrocatalyst is to disperse catalytic metals, such as Pt nanoparticles, onto durable supports [2], such as carbon nanotubes [6–9], doped carbon nanostructures [10,11], conductive diamonds [12], metal oxides [13,14].

To understand the degradation mechanisms is one important issue in searching for durable electrocatalysts and much work has been done on it [2]. The degradation of electrocatalysts in PEM fuel cells can be divided into two aspects [2]: the corrosion of catalyst support and the sintering of catalytic metals (Pt and Pt alloys), and the two factors influence each other: the catalytic metal Pt catalyzes the oxidation of carbon [15], and the oxidation of carbon accelerates Pt sintering [6]. At present, Pt nanoparticles are usually deposited on porous carbon with high specific surface area to produce electrocatalysts. The thermodynamic potential for the electrochemical oxidation of carbon at standard conditions is 0.207 V, which means that the electrochemical corrosion of the carbon is possible above 0.2 V [2]. It is known that, in PEM fuel cells, cathodes usually see electrode potentials of larger than 0.6 V, sometimes even as high as 1.4 V [16,17]. It has been observed that surface oxides [18,19] and CO/CO_2 [20,21] were produced on carbon when carbon materials or carbon-supported catalysts were electrochemically stressed under real or simulated PEM fuel cell

* Corresponding author. Tel.: +1 509 371 6241; fax: +1 509 371 6242.
E-mail address: yuehe.lin@pnl.gov (Y. Lin).

0378-7753/$ – see front matter © 2008 Elsevier B.V. All rights reserved.
doi:10.1016/j.jpowsour.2008.07.008

conditions [22]. When carbon support was gasified into CO/CO_2, Pt nanoparticles detached from the support and lost catalytic activity [22]; if surface oxides were formed on carbon support, the interaction between Pt nanoparticles and the support might be weakened, which makes it easy for Pt nanoparticles to move, accelerating the sintering of Pt [6]. The mechanisms for Pt nanoparticle sintering on carbon support are more complex and more difficult to elucidate than that for carbon corrosion. According to the available reports on the study of the degradation mechanisms, Pt electrocatalysts degrade through several pathways [2]: (i) the loss of Pt from catalytically active sites in PEM fuel cell electrodes, for example, Pt nanoparticles detach from carbon support [22], Pt atoms dissolve and diffuse into Nafion membrane [23] or the liquid electrolyte solution [24], which is called the dissolution/loss process; (ii) Pt nanoparticle size increases due to the coalescence and the dissolution/redeposition process [24]. The degradation of electrocatalysts is largely dependent on the electrochemical stressing conditions. The detailed mechanism is still a controversial topic [2,24].

The investigation on the durability of PEM fuel cell electrocatalysts is a time-consuming and complex task. To test the durability of electrocatalysts in a real normally working PEM fuel cell is inefficient, if not impossible, because the life requirement for PEM fuel cells, thus the electrocatalysts, is, for example, >5000 h for transportation and >40,000 h for stationary application [22]. Therefore, the so-called accelerated degradation test (ADT) is developed [6,20,25], in which the electrocatalysts were held at a constant potential or potential cycling for a certain time scale under a simulated PEM fuel cell condition, and then the degraded electrocatalysts were analyzed to obtain the detailed information to elucidate the nature of the degradation [1,2]. Even though, to test the durability of electrocatalysts usually takes about 100–200 h, especially for studying the durability of catalyst support materials [1]. The current test protocol for electrocatalyst durability study still needs further improvement for fast screening durable candidate materials.

In this research, we studied the degradation behavior of carbon-supported Pt nanoparticle catalyst under various electrochemical stressing conditions with the emphasis on catalyst support corrosion, which is aimed to develop a novel test protocol that can closely mimic PEM fuel cell working conditions for fast screening durable electrocatalyst supports. We choose the standard electrocatalyst, carbon black-supported Pt nanoparticles (Pt/C), so that the findings in this work are widely applicable to other electrocatalyst systems.

2. Experimental

2.1. Preparation of testing electrodes

10 mg carbon-supported Pt catalyst (ETek 20 wt% Pt/C) was dispersed in 5 mL mixed solution of ethanol and 45 μL 5.0 wt% Nafion, and ultrasonicated to form a uniform black ink with the catalyst concentration of 2 mg mL^{-1}. The thin-film rotating disk electrode (TF-RDE) was prepared by applying 6.0 μL of the well-dispersed catalyst ink onto polished glassy-carbon (GC) disk (5 mm in diameter) [26]. After dried at room temperature, the catalyst was well dispersed on the glassy-carbon disk, covering all the surface of glass carbon (Nafion is added in the catalyst layer to closely mimic a real PEM fuel cell condition). The total loading of Pt/C catalyst was 12 μg (2.4 μg Pt). Finally, 10 μL 0.1% Nafion solution was applied onto the surface of the catalyst layer to form a thin film protecting catalyst particles from detaching from the catalyst layer during the long-term test. Before test, the TF-RDE was dried at room temperature overnight.

2.2. Electrochemical test

The Pt/C TF-RDE was first activated with cyclic voltammetry (CV, 0–1.1 V at 50 mV s^{-1}) in Argon gas purged 0.5 M H_2SO_4 solution until a steady CV was obtained. The CV was also used to determine the electrochemical surface area (ESA) of Pt [27,28]. A Pt wire counter-electrode and an Hg/Hg_2SO_4 reference electrode were used in a standard three-electrode electrochemical cell controlled with a CHI660A electrochemical workstation (CH Instruments, Inc., USA).

All the tests were conducted at room temperature. All potentials were reported versus reversible hydrogen electrode (RHE).

2.3. Material characterization

The TEM images of the catalysts were taken using a JEOL TEM 2010 microscope equipped with an Oxford ISIS system. The operating voltage on the microscope was 200 keV. All images were digitally recorded with a slow-scan CCD camera.

The XPS measurements were obtained by the Physical Electronics Quantum 2000 Scanning ESCA Microprobe. This system used a focused monochromatic aluminum Kα X-ray (1486.6 eV) source and a spherical section analyzer. The X-ray beam used was a 100 W, 100-mm diameter beam rastered over a 1.3-mm by 0.2-mm area on the sample. Wide-scan data were collected using a pass energy of 117.4 eV. For the $Ag3d_{5/2}$ line, these conditions produced a full width at half maximum of 1.6 eV. High-energy photoemission spectra were collected using a pass energy of 23.95 eV. For the $Ag3d_{5/2}$ line, these conditions produced a FWHM of 0.80 eV. The binding-energy scale was calibrated using $Cu2p_{3/2}$ at 932.62 ± 0.05 eV and Au 4f at 83.96 ± 0.05 eV.

The samples were dried in vacuum before XPS test.

3. Results and discussions

The durability of PEM fuel cell catalyst support was usually tested with an accelerated degradation protocol in which the catalysts (or only support materials) were held at the fixed-potential of about 1.2 V for a certain time scale in acid solution followed with the characterization of the catalysts (or support materials) [1,2]. By comparing the properties and performance of the catalysts, the degradation information about the catalysts and their support materials can be obtained [6,18,29]. Here, we also tested Pt/C under 1.2 V potential holding for 120 h [donated as Pstat(1.2V)] as reference. To further accelerate the degradation of the catalyst support in order to fast screen the candidate support materials, we employed a more corrosive test method by holding the catalyst at 1.4 V [Pstat(1.4V)]. The potential step with the upper potential of 1.4 V for 150 s and the lower potential limits (0.60 V, 0.85 V) for 30 s in each period was also employed [denoted as Pstep(1.4V_150s–0.60V_30s and Pstep(1.4V_150s–0.85V_30s), respectively]. The upper potential limit was chosen to be 1.4 V due to the following considerations: (1) 1.4 V is close to the PEM fuel cell cathode potential in the condition of the reverse current [16] and local fuel starvation [22,30], at which the corrosion of carbon support is severe; (2) 1.4 V is almost the highest potential without causing oxygen evolution, otherwise the oxygen evolution gas might mechanically detach catalyst particles from the electrode; (3) at 1.4 V, the dissolution of Pt was considered to be suppressed due to the further passivation from Pt surface oxides [31], compared with that in the potential range of 1.1–1.3 V [32]. The lower potential limits of 0.60 V and 0.85 V are close to the cathode potential of normally working PEM fuel cells.

Fig. 1 shows representative TEM images of Pt/C before and after the degradation under various conditions. The TEM image of the original Pt/C (Fig. 1a) shows a high dispersion of Pt nanoparticles.

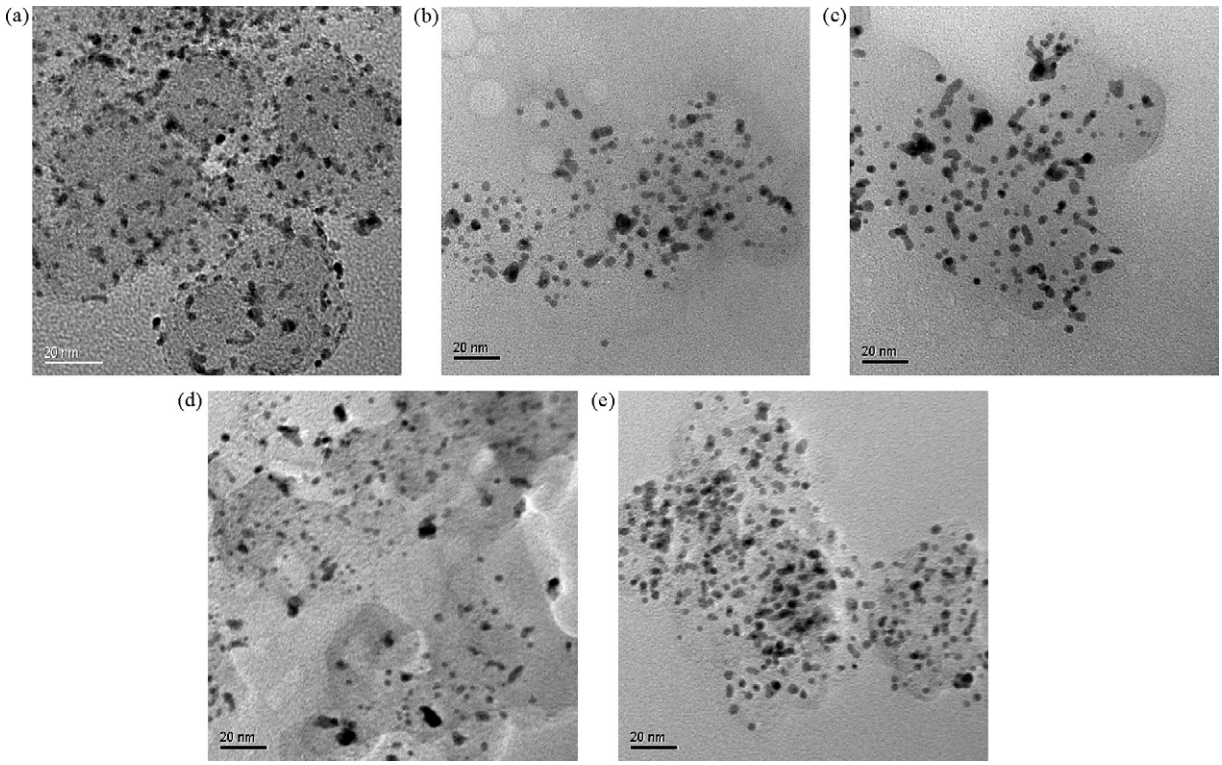

Fig. 1. Representative TEM images of (a) original Pt/C, and the degraded Pt/C under the conditions of (b) Pstat(1.2V)–120h, (c) Pstat(1.4V)–120h, (d) Ptep(1.4V_150s–0.85V_30s)–20h, and (e) Pstep(1.4V_150s–0.60V_30s)–8h. (*Note*: Pstat(1.2V) means "potential-static holding at 1.2 V", Pstep(1.4V_150s–0.85V_30s) means "potential step with the upper potential of 1.4 V for 150 s in each period and the lower potential limit of 0.85 V for 30 s in each period", and so on).

After the degradation, Pt particle sizes increase obviously (Fig. 1b–e); in the image (e), a relatively uniform dispersion of Pt particles is observed with few larger particles compared with those in the image (b), (c), and (d). From TEM images (6–7 images for each sample), the histograms of Pt particle size distribution are obtained and shown in Fig. 2. The volume/area averaged diameters of Pt particles calculated from TEM images [24,29] and the ESA of Pt calculated from hydrogen adsorption/desorption CV in Ar-saturated 0.5 M H_2SO_4 solution [27,28,33] are shown in Table 1. The chemical surface area (CSA, cm^2) of catalysts calculated using the following equation [29,34] is also shown in Table 1.

$$\mathrm{CSA} = \frac{60m}{\rho d}$$

where m is the mass loading of Pt on the electrode, ρ is the density of Pt (21.4 g cm^{-3}) and d (nm) is the calculated volume/area averaged diameter of the Pt particles.

It can be observed from Fig. 2 and Table 1 that, as expected, Pt nanoparticles in original Pt/C sample have a narrow size distribution with an average size of 3.12 nm; Pt particles in the degraded samples under the conditions of (b) Pstat(1.2V)–120h, (c) Pstat(1.4V)–120h, and (d) Pstep(1.4V_150s–0.85V_30s)–20h exhibit a wide size distribution with a distinctive tail toward the large size in the histograms, and the average size of Pt nanoparticles are 4.54 nm, 5.24 nm, and 4.75 nm, respectively. In the case of (e) Pstep(1.4V_150s–0.60V_30s)–8h, Pt particles show an average size of 3.84 nm and the size distribution is wider than that of original sample but narrower than that of the degraded samples under above (b), (c), (d) conditions. It should be noted that the number of Pt nanoparticles smaller than 1.0 nm in the case of (e) was greatly decreased (even smaller Pt nanoparticles disappeared). Table 1 shows that the percentages of the degradation in ESA under the condition of (b), (c) and (d) are almost the same as that in CSA, respectively, which implies that the degradation in the ESA is mainly due to Pt particle size increase in the case of (b), (c) and (d) (see below for details). However, in the case of (e) Pstep(1.4V_150s–0.60V_30s)–8h, the degradation percentage of CSA is only about half of the degradation percentage of ESA, indicating that some factors other than Pt particle size increase contribute to the degradation of ESA.

Even though the detailed mechanism is still a controversial topic, two kinds of processes are considered to contribute to the degradation of Pt catalysts (ESA) [1,2,24,35], which can be summarized as the following: One is the electrochemical process, in which Pt is dissolved to form Pt ions (Pt^{x+}). One part of the dissolved Pt goes into the solution by long-range diffusion (in acid

Table 1
The physical properties of Pt/C electrocatalysts before and after degradation

Test protocol	ESA1 (cm^2)	ESA2 (cm^2)	ESA2 (%)	d1 (nm)	d2 (nm)	CSA1 (cm^2)	CSA2 (cm^2)	CSA2 (%)
Pstat(1.2V)–120h	2.11	1.49	70.6	3.12	4.54	2.156	1.48	68.7
Pstat(1.4V)–120h	2.17	1.26	58.2	3.12	5.24	2.156	1.28	59.5
Pstep(1.4–0.85V)–20h	1.96	1.27	64.8	3.12	4.75	2.156	1.42	65.7
Pstep(1.4–0.60V)–8h	2.01	1.22	60.5	3.12	3.84	2.156	1.75	81.2

Note: Pt loading 2.4 μg. ESA1, d1 and CSA1 are, respectively the electrochemical surface area, the volume/area averaged diameter from TEM images, and chemical surface area of original samples, and the ESA2, d2, and CSA2 are the corresponding values of the post-degradation samples.

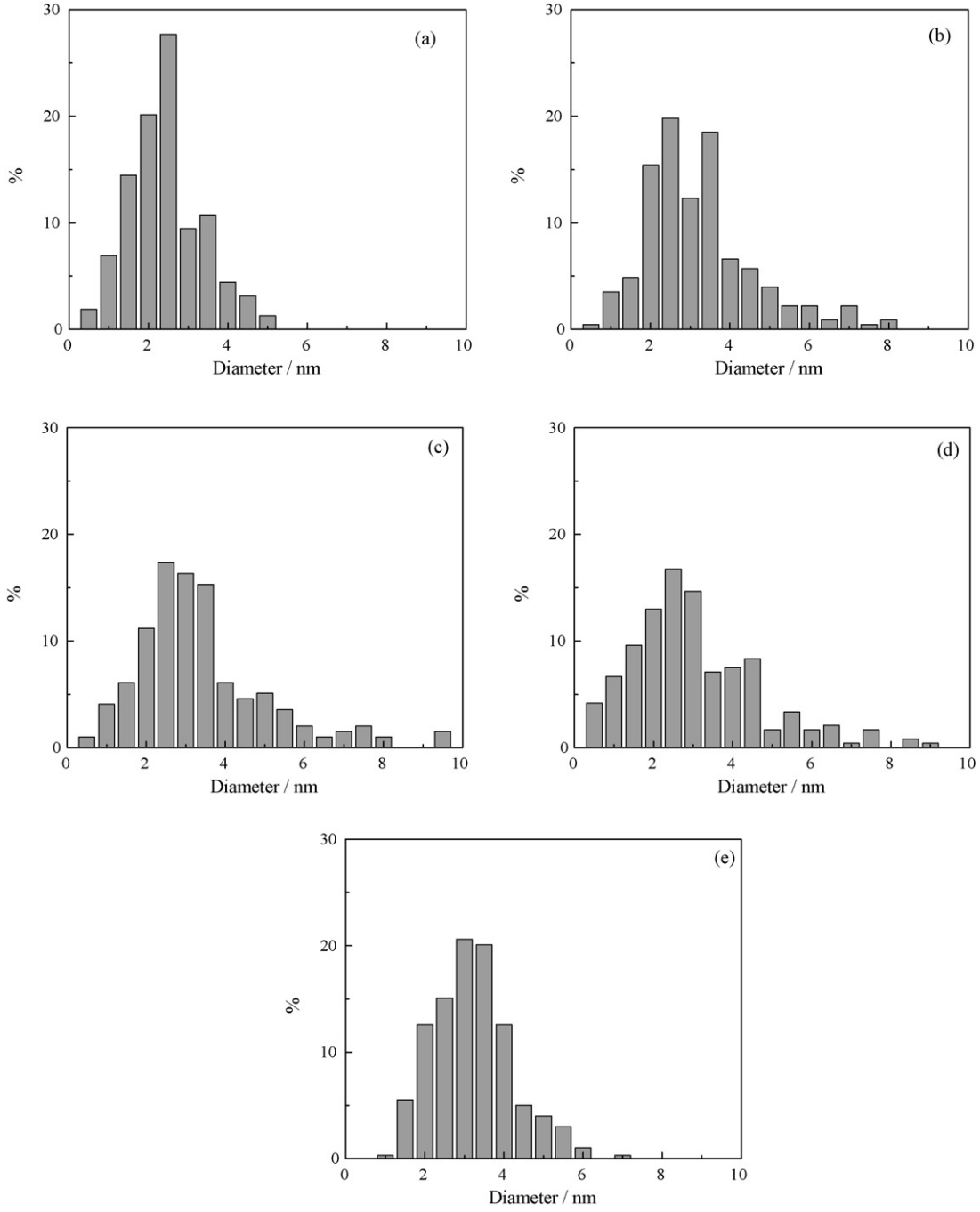

Fig. 2. Histograms of Pt nanoparticle size distribution for the samples before and after the degradation under various conditions: (a) original Pt/C, and the degraded Pt/C under the conditions of (b) Pstat(1.2V)–120h, (c) Pstat(1.4V)–120h, (d) Ptep(1.4V_150s–0.85V_30s)–20h, and (e) Pstep(1.4V_150s–0.60V_30s)–8h.

solution test condition) or into the PEM (in a real PEM fuel cell test condition), the other part of the dissolved Pt ions near the surface of Pt particles redeposit onto Pt particles; the dissolution of Pt usually occurs at high electrode potentials and the redeposition usually takes place at low potentials. The dissolution/redeposition contributes to Pt particle size increase. The other kind of process is the physical one, which includes several situations: the first one is the migration/coalescence process of Pt nanoparticles on support surface, which contributes to Pt particle size increase; the second one is that Pt nanoparticles detached from catalyst support, one part of the detached Pt particles leave the support and lose activity, the other part of the detached Pt particles, which are very close to each other, might coalesce to form large particles. If the migration/coalescence process is the main reason for the degradation of the catalyst, the degradation in ESA and CSA should be almost the same because the contributing factors (Pt particle size increase) for the degradation of the ESA and the CSA are the same, which corresponds to (b), (c) and (d) in Figs. 1 and 2; if Pt dissolution is prominent, whether part of it redeposit onto Pt particles or not, the degradation percentage in ESA should be larger than that for CSA due to the net loss of Pt from the electrode, as observed in the case of (e). Pt particle shape and particle size distribution of the degraded catalyst should also be different for the migration/coalescence and the dissolution/redeposition

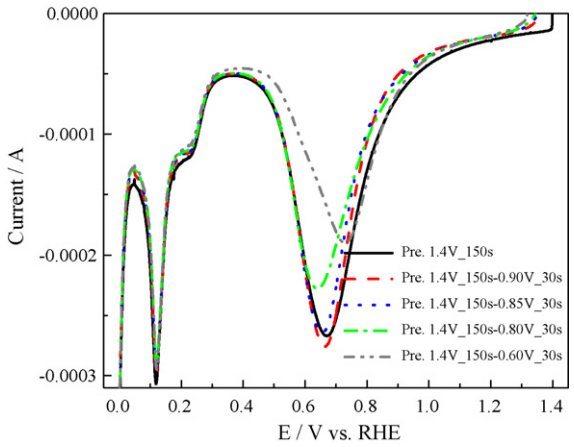

Fig. 3. The linear sweep voltammetry (LSV) on Pt/C electrocatalyst electrodes with various preconditionings ("Pre. 1.4V_150s" means "preconditioned at 1.4 V for 150 s"; "Pre. 1.4V_150s–0.90V_30s" means "preconditioned using the potential step with the upper potential of 1.4 V for 150 s and the lower potential limit of 0.90 V for 30 s"; and so on).

mechanisms [2,24,35]: the former process usually produces Pt particles with a non-spherical shape and much larger particles, and the size distribution is wide (with a tail at large size), as observed in (b), (c), (d) in Figs. 1 and 2; and the dissolution/redeposition process usually produces spherically shaped Pt particle and the size distribution is narrow with the number of smaller particle greatly decreased or disappeared, both of which are due to the tendency of minimizing surface energy, which corresponds to the case of (e) in Figs. 1 and 2. By comparing the TEM images, the size distribution and the degradation percentage in ESA and CSA of each samples, it is reasonable to propose that the degradation mechanisms of Pt/C under the condition of Pstat(1.2V)–120h, Pstat(1.4V)–120h and Pstep(1.4V_150s–0.85V_30s)–20h are similar which are mainly due to the migration/coalescence process, so they are almost equal in evaluating the durability of electrocatalysts; the degradation of Pt/C under Pstep(1.4V_150s–0.60V_30s)–8h condition is mainly due to the dissolution/loss and the dissolution/redeposition mechanism (the migration/coalescence mechanism cannot be completely excluded).

In order to get an elucidation of the underlying reasons for the different degradation mechanisms, we carried out the linear sweep voltammetry (LSV) on Pt/C electrode with various preconditioning, as shown in Fig. 3. A clear reduction current peak can be observed around 0.70 V in the LSV, which is due to the reduction of Pt surface oxides. For the samples preconditioned at Pstat(1.4V_150s), Pstep(1.4V_150s–0.90V_30s) and Pstep(1.4V_150s–0.85V_30s), the reduction peaks were similar, and for Pstep(1.4V_150s–0.80V_30s) and Pstep(1.4V_150s–0.60V_30s), the reduction peaks were greatly suppressed. This indicates: when the electrode was held at 1.4V_150s, surface oxides were formed on Pt particle surface; when the electrode potential was stepped from 1.4 V to the potentials above 0.85 V (0.90V_30s and 0.85V_30s), surface oxides were rarely reduced, while a relatively larger amount of Pt surface oxides were reduced when the electrode was stepped to the potentials below 0.85 V (0.80V_30s and 0.60V_30s). This means that, under the condition of Pstep(1.4V_150s–0.85V_30s) and Pstep(1.4V_150s–0.90V_30s), Pt surface was constantly passivated by surface oxides, so the dissolution of Pt was greatly suppressed [32]; under the condition of Pstep(1.4V_150s–0.60V_30s), the electrode was periodically switched between passivated state and activated state, i.e., when the electrode was switched to 0.60 V, Pt surface oxides were reduced and freshly produced Pt atoms covered the surface of Pt particles, the subsequent switch of the electrode potential to 1.4 V (in the sequent potential step) leads to Pt dissolution until Pt surface was repassivated. The cycle of passivation/activation (oxidation/reduction) of Pt particles during Pstep(1.4V_150s–0.60V_30s) accelerated Pt dissolution and redeposition [32].

The degradation rate of Pt/C was enhanced under Ptep(1.4V_150s–0.85V_30s) condition as compared with that under the condition of potential-static holding at 1.4 V even though the degradation mechanisms are similar under these conditions. We need to make a study on why the degradation rate is accelerated under potential step condition.

Fig. 4 presents the *i*–*t* plots of Pt/C electrode under the conditions of Pstat(1.4V) and Pstep(1.4V_150s–0.85V_30s). It can be seen that the oxidation current under potential step condition (if averaged) is much larger than that under potential-static condition (the fast charging due to the electrochemical double layer can be limited to the first few seconds in each period), which means the oxidation of carbon support was accelerated under Pstep(1.4V_150s–0.85V_30s) condition.

Pt/C before and after the degradation were characterized with XPS, which tells the total surface oxygen content of carbon support: the higher the surface oxygen content, the higher the oxidation degree of carbon support [6,18,19,36]. Fig. 5 show that wide-scan XPS spectra and the surface oxygen content, which was calculated using the high-energy XPS (C1s and O1s) [6]. It clearly shows that the surface oxygen content increases from 3.3% to 8.8% and 12.5% for the sample after the degradation under potential-static condition and potential step condition, respectively. Fig. 6 shows that C1s spectra of each sample. The shoulder in the binding-energy range of carbon bound with surface oxygen was enhanced after degradation, which is higher for the potential step condition. XPS data shows that the oxidation of carbon support was accelerated under potential step condition. Carbon support could also be oxidized into CO_2/CO under the degradation conditions [2,21], but the amount of CO_2/CO was too small to be measured due to the very low loading of catalysts on the TF-RDE. The electrochemical *i*–*t* plots and XPS were employed to

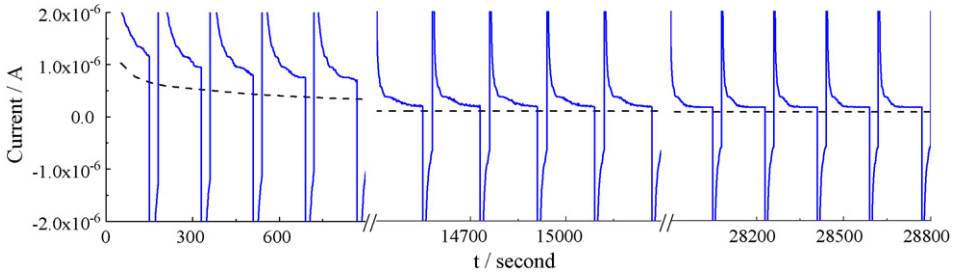

Fig. 4. The *i*–*t* plots of Pt/C electrodes under the conditions of Pstat(1.4V) (dashed black) and Pstep(1.4V_150s–0.85V_30s) (solid blue). (For interpretation of the references to color in the figure caption, the reader is referred to the web version of the article.)

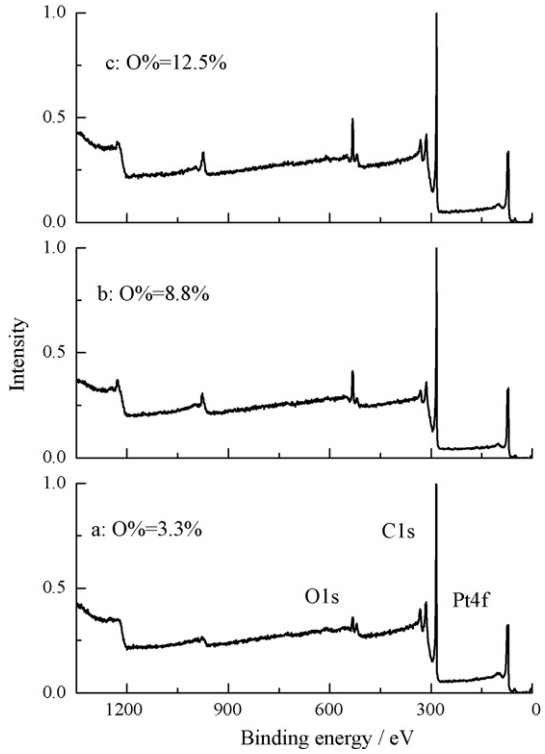

Fig. 5. The wide-scan XPS spectra of Pt/C electrocatalysts before (a) and after the degradation under the conditions of (b) Pstat(1.4V)–120h and (c) Pstep(1.4V_150s–0.85V_30s)–20h.

study the oxidation of carbon support which gave the same conclusion on the influence of electrochemical stressing conditions on the oxidation of carbon support: the electrochemical stressing condition with potential step accelerated the corrosion of carbon support in Pt/C. This might be the main reason that the degradation rate of Pt/C is higher under Pstep(1.4V_150s–0.85V_30s) than that under Pstat(1.4V) although they are under the similar degradation mechanisms.

These findings can be employed to develop a novel test protocol for fast screening durable catalyst support. As stated above, to test the durability of catalyst and support in a real normally working PEM fuel cell is inefficient. To hold the supported catalyst or the pure support material at a fixed-potential (usually 1.0–1.2 V RHE) is the most widely used approach to study the support durability [6,19,29,37,38], but it takes several days or more to observe the obvious degradation of the catalyst. For example, as shown in Table 1, to degrade the ESA of the catalysts by ~30% takes 120 h (one week) if using Pstat(1.2V) method, but less than 20 h is required if using our Pstep(1.4V_150s–0.85V_30s) method. As shown above, these two methods are equal in evaluating the durability of catalyst support. The Pstep(1.4V_150s–0.85V_30s) method can be employed to replace the widely used potential-static holding method [1,2] in fast screening durable catalyst support materials.

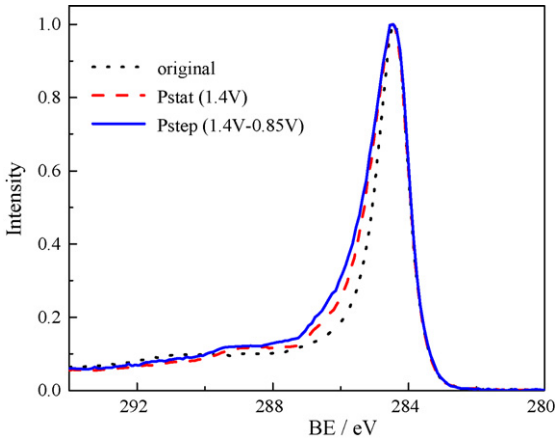

Fig. 6. High-energy C1s XPS spectra of Pt/C electrocatalysts before and after the degradation under various conditions.

4. Conclusions

To elucidate the mechanisms for the degradation of electrocatalysts is very important for developing durable electrocatalysts for PEM fuel cell. The degradation of Pt/C depends on the electrochemical stressing conditions, in terms of both degradation rates and mechanisms. Pt/C electrocatalysts degrade faster under potential step conditions [Pstep(1.4V_150s–0.85V_30s) and Pstep(1.4V_150s–0.60V_30s)] than that under potential-static holding conditions (1.2 V and 1.4 V), which is attributed to the enhanced corrosion of carbon support under Pstep(1.4V_150s–0.85V_30s) and the enhanced dissolution of Pt under Pstep(1.4V_150s–0.60V_30s). The degradation mechanisms for Pt/C under the conditions of Pstep(1.4V_150s–0.85V_30s) and potential-static holding at 1.2 V and 1.4 V are similar, which is through the coalescence process. They are almost equal in evaluating the durability of electrocatalyst support materials. And the degradation of Pt/C under Pstep(1.4V_150s–0.60V_30s) is mainly through the dissolution/loss and dissolution/redeposition process. The difference in the degradation mechanisms is attributed to the chemical states of Pt nanoparticles: Pt dissolution was alleviated by the protective oxide layer under Pstep(1.4V_150s–0.85V_30s). The electrochemical stressing method of Pstep(1.4V_150s–0.85V_30s) can be used for fast screening durable catalyst support materials.

Acknowledgement

This work is supported by the U.S. DOE-EERE Hydrogen Program. The research described in this paper was performed at the Environmental Molecular Science Laboratory, a national scientific used facility sponsored by DOE's Office of Biological and Environmental Research and located at Pacific Northwest National Laboratory (PNNL). PNNL is operated by Battelle for DOE under Contract DE-AC05-76L01830. Authors would like to acknowledge Mr. Mark Engelhard for XPS measurement and Dr. Chongmin Wang for TEM measurement.

References

[1] R. Borup, J. Meyers, B. Pivovar, Y.S. Kim, R. Mukundan, N. Garland, D. Myers, M. Wilson, F. Garzon, D. Wood, P. Zelenay, K. More, K. Stroh, T. Zawodzinski, J. Boncella, J.E. McGrath, M. Inaba, K. Miyatake, M. Hori, K. Ota, Z. Ogumi, S. Miyata, A. Nishikata, Z. Siroma, Y. Uchimoto, K. Yasuda, K.I. Kimijima, N. Iwashita, Chem. Rev. 107 (2007) 3904–3951.
[2] Y. Shao, G. Yin, Y. Gao, J. Power Sources 171 (2007) 558–566.
[3] Y. Shao, G. Yin, Z. Wang, Y. Gao, J. Power Sources 167 (2007) 235–242.
[4] J. Zhang, K. Sasaki, E. Sutter, R.R. Adzic, Science 315 (2007) 220–222.
[5] V.R. Stamenkovic, B. Fowler, B.S. Mun, G.F. Wang, P.N. Ross, C.A. Lucas, N.M. Markovic, Science 315 (2007) 493–497.
[6] Y.Y. Shao, G.P. Yin, Y.Z. Gao, P.F. Shi, J. Electrochem. Soc. 153 (2006) A1093–A1097.
[7] X. Wang, W.Z. Li, Z.W. Chen, M. Waje, Y.S. Yan, J. Power Sources 158 (2006) 154–159.
[8] X.R. Ye, Y.H. Lin, C.M. Wang, M.H. Engelhard, Y. Wang, C.M. Wai, J. Mater. Chem. 14 (2004) 908–913.
[9] Y.H. Lin, X.L. Cui, C.H. Yen, C.M. Wai, Langmuir 21 (2005) 11474–11479.
[10] Y. Shao, J. Sui, G. Yin, Y. Gao, Appl. Catal. B: Environ. 79 (2008) 89–99.
[11] G. Wu, D.Y. Li, C.S. Dai, D.L. Wang, N. Li, Langmuir 24 (2008) 3566–3575.
[12] A.E. Fischer, G.M. Swain, J. Electrochem. Soc. 152 (2005) B369–B375.
[13] H. Chhina, S. Campbell, O. Kesler, J. Power Sources 161 (2006) 893–900.

[14] M.S. Saha, R.Y. Li, M. Cai, X.L. Sun, Electrochem. Solid State Lett. 10 (2007) B130–B133.
[15] Z. Siroma, K. Ishii, K. Yasuda, Y. Miyazaki, M. Inaba, A. Tasaka, Electrochem. Commun. 7 (2005) 1153–1156.
[16] C.A. Reiser, L. Bregoli, T.W. Patterson, J.S. Yi, J.D.L. Yang, M.L. Perry, T.D. Jarvi, Electrochem. Solid State Lett. 8 (2005) A273–A276.
[17] H. Tang, Z.G. Qi, M. Ramani, J.F. Elter, J. Power Sources 158 (2006) 1306–1312.
[18] Y.Y. Shao, G.P. Yin, J. Zhang, Y.Z. Gao, Electrochim. Acta 51 (2006) 5853–5857.
[19] K.H. Kangasniemi, D.A. Condit, T.D. Jarvi, J. Electrochem. Soc. 151 (2004) E125–E132.
[20] K. Teranishi, K. Kawata, S. Tsushima, S. Hirai, Electrochem. Solid State Lett. 9 (2006) A475–A477.
[21] L.M. Roen, C.H. Paik, T.D. Jarvic, Electrochem. Solid State Lett. 7 (2004) A19–A22.
[22] S.D. Knights, K.M. Colbow, J. St-Pierre, D.P. Wilkinson, J. Power Sources 127 (2004) 127–134.
[23] W. Bi, G.E. Gray, T.F. Fuller, Electrochem. Solid State Lett. 10 (2007) B101–B104.
[24] P.J. Ferreira, G.J. La, O.Y. Shao-Horn, D. Morgan, R. Makharia, S. Kocha, H.A. Gasteiger, J. Electrochem. Soc. 152 (2005) A2256–A2271.
[25] H.R. Colon-Mercado, H. Kim, B.N. Popov, Electrochem. Commun. 6 (2004) 795–799.
[26] U.A. Paulus, T.J. Schmidt, H.A. Gasteiger, R.J. Behm, J. Electroanal. Chem. 495 (2001) 134–145.
[27] Y.Y. Shao, G.P. Yin, J.J. Wang, Y.Z. Gao, P.F. Shi, J. Electrochem. Soc. 153 (2006) A1261–A1265.
[28] Y.Y. Shao, G.P. Yin, J.J. Wang, Y.Z. Gao, P.F. Shi, J. Power Sources 161 (2006) 47–53.
[29] L. Li, Y.C. Xing, J. Electrochem. Soc. 153 (2006) A1823–A1828.
[30] T.W. Patterson, R.M. Darling, Electrochem. Solid State Lett. 9 (2006) A183–A185.
[31] V.A.T. Dam, F.A. de Bruijn, J. Electrochem. Soc. 154 (2007) B494–B499.
[32] X.P. Wang, R. Kumar, D.J. Myers, Electrochem. Solid State Lett. 9 (2006) A225–A227.
[33] A. Pozio, M. De Francesco, A. Cemmi, F. Cardellini, L. Giorgi, J. Power Sources 105 (2002) 13–19.
[34] W.M. Chen, G.Q. Sun, J.S. Guo, X.S. Zhao, S.Y. Yan, J. Tian, S.H. Tang, Z.H. Zhou, Q. Xin, Electrochim. Acta 51 (2006) 2391–2399.
[35] Y. Shao-Horn, W.C. Sheng, S. Chen, P.J. Ferreira, E.F. Holby, D. Morgan, Top. Catal. 46 (2007) 285–305.
[36] J.L. Figueiredo, M.F.R. Pereira, M.M.A. Freitas, J.J.M. Orfao, Carbon 37 (1999) 1379–1389.
[37] M.F. Mathias, R. Makharia, H.A. Gasteiger, J.J. Conley, T.J. Fuller, C.J. Gittleman, S.S. Kocha, D.P. Miller, C.K. Mittelsteadt, T. Xie, S.G. Yan, P.T. Yu, Interface 14 (2005) 24–35.
[38] S. Ball, S. Hudson, B. Theobald, D. Thompsett, ECS Trans. 3 (2006) 595–605.